Coherent Storage and Phase Modulation of Single Hard-X-Ray Photons Using Nuclear Excitons

Wen-Te Liao,* Adriana Pálffy,† and Christoph H. Keitel
Max-Planck-Institut für Kernphysik, Saupfercheckweg 1, D-69117 Heidelberg, Germany
(Received 2 May 2012; published 9 November 2012)

The coherent storage and phase modulation of x-ray single-photon wave packets in the resonant scattering of light off nuclei is theoretically investigated. We show that by switching off and on again the magnetic field in the nuclear sample, phase-sensitive storage of photons in the keV regime can be achieved. Corresponding π phase modulation of the stored photon can be accomplished if the retrieving magnetic field is rotated by 180°. The development of such x-ray single-photon control techniques is a first step towards forwarding quantum optics and quantum information to shorter wavelengths and more compact photonic devices.

DOI: 10.1103/PhysRevLett.109.197403 PACS numbers: 78.70.Ck, 42.50.Md, 42.50.Nn, 76.80.+y

Finding versatile solutions for quantum and classical computing on the most compact scale is one of the crucial objectives in both fundamental physics and information technology. The photon as flying qubit is anticipated to be the fastest information carrier and to provide the most efficient computing implementation. However, with the extension of Moore's law [1] to the future, quantum photonic circuits must meet the bottleneck of the diffraction limit, i.e., a few hundred nm for the optical region. Forwarding optics and quantum information to shorter wavelengths in the x-ray region has the potential of shrinking computing elements in future photonic devices such as the quantum photonic circuit [2]. This is strongly related to the development and availability of compact x-ray sources based on tabletop plasma wigglers [3] and magnet undulators [4] or x-ray high-harmonic generation with optical coherent light sources [5]. The realization of a short wavelength quantum photonic circuit requires mastery of x-ray optics and powerful control tools of single-photon wave packet amplitude, frequency, polarization, and phase [6]. The development of x-ray optics elements has already made significant progress with the realization of x-ray diamond mirrors [7–9] and cavities [10], hard-x-ray waveguides [11,12], and the Fabry-Pérot resonator [13–15]. Efficient coherent photon storage for photon delay lines and x-ray phase modulation, preferably even for single-photon wave packets, are the next milestones to be reached.

Moving towards the interactions in the x-ray regime [16–21], new physical systems also come into play; e.g., nuclei with low-lying collective states naturally arise as candidates for x-ray quantum optics studies. Nuclear quantum optics [22–24] and nuclear coherent population transfer [25] are rendered experimentally possible by the advent and commissioning of x-ray free electron lasers (XFEL) [26–28]. Coherent control tools based on nuclear cooperative effects [29–33] are known also from nuclear forward scattering (NFS) experiments with third-generation synchrotron light sources. The underlying physics here relies on the delocalized nature of the nuclear excitation produced by coherent XFEL or synchrotron radiation (SR) light, i.e., the formation of so-called nuclear excitons. A key example in this direction is how the manipulation of the hyperfine magnetic field in NFS systems provides the means to store nuclear excitation energy [34] and in turn to generate keV single-photon entanglement [35].

In this Letter, we present two important control tools for single hard-x-ray photons using resonant scattering of light off nuclei in an NFS setup. The formation of a nuclear exciton consisting of a single delocalized excitation opens the possibility to control the coherent decay and therefore emission of the scattered photon. Making use of this feature, we first put forward how to coherently store a single hard-x-ray photon for time intervals of 10–100 ns by turning off the hyperfine magnetic field in an NFS system. The stored single photon can be released by turning on the magnetic field. We emphasize that our scheme conserves not only the excitation energy, as already pioneeringly demonstrated in Ref. [34], but also the photonic polarization and phase beyond the ps time range. Next, we show how to modulate the stored photon with a phase shift of π by using a releasing hyperfine magnetic field oriented in the opposite direction to the initial one. For the measurement of this π phase shift of the retrieved photon, we refer to the echo technique using two nuclear targets [36–38] and demonstrate for the first time a magnetically induced nuclear exciton echo without any mechanical vibration of the targets. This feasible echo two-sample setup can also be used for phase-sensitive photon storage involving a mere rotation of the hyperfine magnetic field by 180°.

The typical NFS setup involves a solid-state target containing ^{57}Fe. An x-ray pulse with meV bandwidth (either SR or coherent XFEL light) tuned on the 14.413 keV nuclear transition from the ground state to the first excited state shines perpendicular to the nuclear sample, as shown in Fig. 1(a). SR typically produces at most one excited nucleus per pulse, thus providing a reliable single excitation and single released photon scenario. The disadvantage here is that the initial photonic phase is undefined.

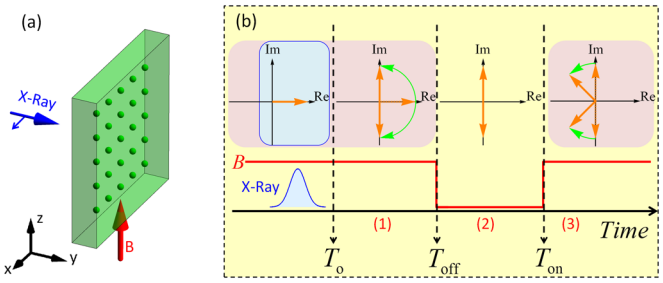

FIG. 1 (color online). (a) NFS setup. The linear polarized x-ray pulse propagates in the y direction, and **B** is the external magnetic field initially parallel to the z axis. (b) Time dependence of the hyperfine magnetic field **B** and the corresponding dynamics of the nuclear currents (rotating arrows). The dynamics will be surveyed in three temporal domains: (1) $T_o < t < T_{off}$; (2) $T_{off} < t < T_{on}$; (3) $T_{on} < t$.

Coherent x-ray light from seeded or oscillator XFEL [39–41] with a well-defined photonic phase can be used at low intensities such as to keep the excitation rate below one nucleus per pulse in the sample and guarantee single photons. Control over the number of excited nuclei per pulse can be achieved either by using x-ray partial reflection or partial transmission on silicon mirrors [7] to limit the laser beam intensity or by varying the concentration of ^{57}Fe nuclei in the target. An externally applied magnetic field **B** parallel to the z axis induces the nuclear hyperfine splitting of the ground and excited ^{57}Fe nuclear states of spins $I_g = 1/2$ and $I_e = 3/2$, respectively. Depending on the pulse polarization, different hyperfine transitions will be driven. In the following, we consider the x-ray field linearly polarized parallel to the x axis driving the two $\Delta m = m_e - m_g = 0$ magnetic dipole transitions, where m_e and m_g denote the projections of the excited and ground state nuclear spins on the quantization axis, respectively.

The dynamics of the density matrix $\hat{\rho}$ is governed by the Maxwell-Bloch equations [42–45]

$$\begin{aligned} \partial_t \hat{\rho} &= \frac{1}{i\hbar}[\hat{H}, \hat{\rho}] + \hat{\rho}_s, \\ \frac{1}{c}\partial_t \Omega + \partial_y \Omega &= i\eta(a_{31}\rho_{31} + a_{42}\rho_{42}), \end{aligned} \tag{1}$$

with the interaction Hamiltonian

$$\hat{H} = -\frac{\hbar}{2} \times \begin{pmatrix} 2\Delta_g & 0 & a_{13}\Omega^* & 0 \\ 0 & -2\Delta_g & 0 & a_{24}\Omega^* \\ a_{31}\Omega & 0 & -2(\Delta + \Delta_e) & 0 \\ 0 & a_{42}\Omega & 0 & -2(\Delta - \Delta_e) \end{pmatrix}.$$

In the equations above, Δ is the x-ray detuning to the 14.4 keV transition assumed to be zero and $\Delta_{g(e)}$ denotes the Zeeman energy splitting of the nuclear ground (excited) state proportional to the magnetic field **B**. In Eq. (1), $\rho_{eg} = A_e A_g^*$ for $e \in \{1, 2\}$ and $g \in \{3, 4\}$ are the density matrix elements of $\hat{\rho}$ for the nuclear wave function $|\psi\rangle = A_1|1\rangle + A_2|2\rangle + A_3|3\rangle + A_4|4\rangle$. The ket vectors are the eigenvectors of the two ground and two excited states hyperfine levels with $m_g = -1/2$, $m_g = 1/2$, $m_e = -1/2$, and $m_e = 1/2$, respectively. Furthermore, $a_{eg} = a_{ge} = \sqrt{2/3}$ are the corresponding Clebsch-Gordan coefficients [45,46] for the $\Delta m = 0$ transitions, and $\hat{\rho}_s$ describes the spontaneous decay [44]. The parameter η is defined as $\eta = \frac{6\Gamma}{L}\alpha$, where $\Gamma = 1/141.1$ GHz is the spontaneous decay rate of excited states, α represents the effective resonant thickness [42,43,46], and $L = 10$ μm the thickness of the target. Further notations are Ω for the Rabi frequency, which is proportional to the electric field $\vec{E}$ of the x-ray pulse [44,45], and c, the speed of light.

Figure 1(b) illustrates the time evolution of our photon storage scheme. The external magnetic field **B**, depicted by the red line, is present before the x-ray pulse impinges on the target at T_o. At T_{off} the **B** field is turned off and later turned back on at T_{on}. The rotating orange arrows depict the time evolution of the nuclear transition current matrix elements as defined in Ref. [34]. In our treatment, this is equivalent with investigating the coherence terms $i\rho_{42}$ and $i\rho_{31}$ [42,43]. Initially, the ensemble of ^{57}Fe nuclei is excited by the x-ray pulse at T_o. Subsequently, the purely real currents are abruptly built. In the time interval (1), the two currents start to rotate in opposite directions on the complex plane with the factor of $e^{\pm i\Delta_B t}$ caused by the magnetic field until $t = T_{off}$ when **B** is turned off. The corresponding phase gain is $\pm\Delta_B\tau$. Here and in the following we have used for simplicity the notations $\Delta_B = \Delta_g + \Delta_e$ and $\tau = T_{off} - T_o$. Within the time interval (2), the quantum beat (arising from the interference between the two $\Delta m = 0$ transitions) is frozen with the factor of $e^{\pm i\Delta_B\tau}$ since the hyperfine field has vanished, and only the dynamical beat [29,42,46] due to interference between multiple scattering processes in the sample persists. During the time interval (3), the presence of the magnetic field makes the quantum beat emerge again.

We numerically solve Eq. (1) with $\alpha = 10$ and $\Delta_B = 15\Gamma$ and present our results in Figs. 2 and 3. The NFS signal intensities $|\vec{E}(t, L)|^2$ are compared with the spontaneous decay curves $e^{-\Gamma t}$ and the pure dynamical beat (for the case of no hyperfine splitting) $[\frac{\alpha}{\sqrt{\alpha\Gamma t}} J_1(2\sqrt{\alpha\Gamma t})]^2 e^{-\Gamma t}$ [42,47], where J_1 is the Bessel function of first kind. Figure 2(a) shows the unperturbed NFS time spectrum where both quantum beat and dynamical beat are observed. In Fig. 2(b) we demonstrate photon storage by turning off the magnetic field at $t = 21$ ns (corresponding to a quantum beat minimum, $\Delta_B\tau = \pm N\frac{\pi}{2}$ with N odd). Both nuclear currents corresponding to the $\Delta m = 0$ transitions are frozen on the imaginary axis [see Fig. 1(b)] and undergo destructive interference. In this case, the intensity of the emitted radiation is suppressed by 3 orders of

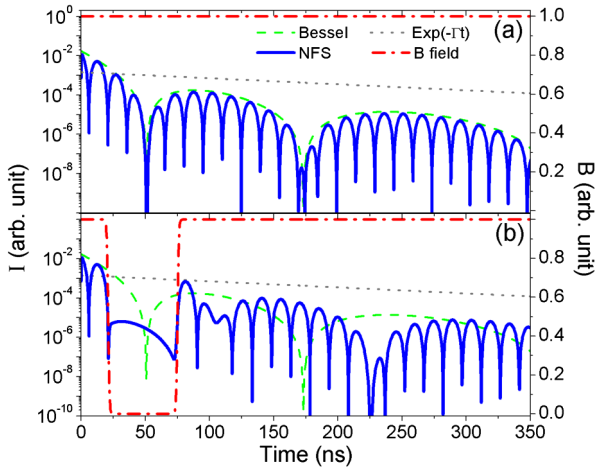

FIG. 2 (color online). (a) Unperturbed NFS time spectrum: blue solid lines are the intensities of the NFS signal, red dash-dotted lines qualitatively denote the applied magnetic field **B**, the gray dotted lines are proportional to $e^{-\Gamma t}$, and the green dashed lines illustrate the dynamical beat [42,47]. (b) The hyperfine magnetic field is turned off at $t = 21$ ns and turned back on at $t = 75$ ns.

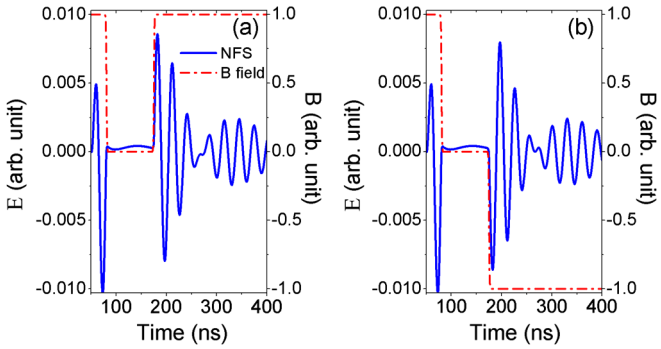

FIG. 3 (color online). Phase modulation of retrieved x-ray via reversing the applied magnetic field **B**. Blue solid lines are the electric field of the NFS signal, and the red dotted-dashed lines denote the applied magnetic fields **B**. The **B** field is turned off at $T_{\rm off} = 80.5$ ns and then switched on at $T_{\rm on} = 175$ ns, such that (a) $\mathbf{B}(t < T_{\rm off}) = \mathbf{B}(t > T_{\rm on})$ and (b) $\mathbf{B}(t < T_{\rm off}) = -\mathbf{B}(t > T_{\rm on})$.

magnitude. Later on, by turning the hyperfine magnetic field on again at $t = 75$ ns, the unsuppressed photon signal is observed again within the time interval (3). Figure 2 also shows that the stored nuclear excitation energy experiences spontaneous decay during the storage time [34].

The electric field envelopes of the scattered photon are presented in Fig. 3. In Fig. 3(a), the magnetic field before $T_{\rm off} = 80.5$ ns and that after $T_{\rm on} = 175$ ns are the same and the phase before storage and after retrieving is continuous. If, however, the retrieving magnetic field is applied in opposite direction, as shown in Fig. 3(b), the phase of the released photonic wave packet will be modulated with a shift of π. This is caused by the effect of reversed time related with the change of sign of the hyperfine magnetic field [48,49]; i.e., all the nuclear currents evolve backwards in time. Our density matrix calculations have been double-checked by the comparison with results from the iterative solution of the wave equations developed in Ref. [34]. The agreement is complete for both electric field envelope and scattered light intensity, proving the equivalence of the two methods.

The most significant advantage of our scheme is the conservation of the photonic polarization and phase. Storage of nuclear excitation energy by magnetic field rotations in NFS experiments with SR was presented in Ref. [34]. This pioneering work opened the avenue of coherent control applications with nuclei using magnetic switching. However, the scheme in Ref. [34] is not phase-sensitive. Since the magnetic Hamiltonian is not zero during the storage, neither the polarization [50] nor the phase of the particular polarization components can be stored, and the properties of the released photon depend on the switching instants. With the advent of coherent XFEL sources and x-ray quantum optics and quantum information experiments, phase storage and modulation become crucial for many applications. So far, the coherent trapping of hard x-rays in crystal cavities provides photon storage for time intervals in the ps range [10]. Our scheme provides robust phase and polarization storage of the x-ray photon on the 10–100 ns scale determined by the nuclear lifetime.

In order to implement our phase-sensitive storage scheme experimentally, a material with no intrinsic nuclear Zeeman splitting such as stainless-steel $Fe_{55}Cr_{25}Ni_{20}$ [36,37] is required. The remaining challenge is to turn off and on the external magnetic fields of a few teslas on the ns time scale. According to our calculations for the case of Fig. 2, the raising time of the **B** field should be shorter than 50 ns (the raising time was considered 4 ns for all presented cases). This could be achieved by using small single- or few-turn coils and a moderate pulse current of ca. 15 kA from low-inductive high-voltage *snapper* capacitors [51]. Another mechanical solution, e.g., the lighthouse setup [52], could be used to move the excited target out of and into a region with confined static **B** field. The sample is first excited while located in a first confined static magnetic field region. A fast rotation moves the sample out of this magnetic field region and later on brings it under the action of a second static magnetic field. Simple geometrical considerations show that a displacement of the size of the sample thickness (about 3.5 μm) corresponds to a time interval of 10 ns at a rotation frequency of 70 kHz and rotor radius of 5 mm [52]. The sample can be thus rotated out of the confined magnetic field region fast enough to provide switching times on the order of 10 ns.

Let us now turn to the measurement of the π phase shift. A typical x-ray optics setup would require letting the π-modulated photon interfere with a part of the original pulse on a triple Laue interferometer [53,54]. We adopt here

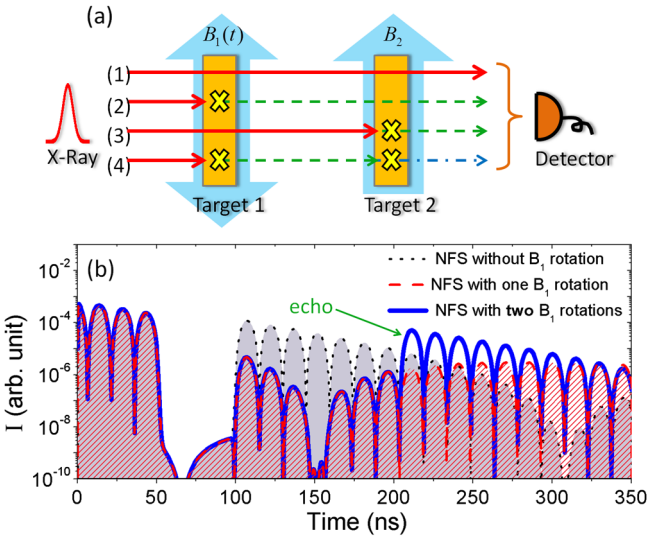

FIG. 4 (color online). (a) Magnetically induced nuclear exciton echo setup with two targets. Yellow crosses illustrate the formation of the nuclear exciton. The light blue vertical wide arrows show the applied magnetic fields: the dynamical $\mathbf{B}_1(t)$ is applied to target 1, whereas the static $\mathbf{B}_2$ is applied to target 2. (b) NFS time spectrum for $\alpha_1 = \alpha_2 = 1$ and $|\Delta_{B1}| = \Delta_{B2} = 15\Gamma$. The magnetic field $\mathbf{B}_1(t)$ is turned off at $T_{\text{off}} = 51$ ns and on at $T_{\text{on}} = 100$ ns. Black dotted line, $\mathbf{B}_1(t > T_{\text{on}}) = \mathbf{B}_1(t < T_{\text{off}})$; red dashed line, $\mathbf{B}_1(t > T_{\text{on}}) = -\mathbf{B}_1(t < T_{\text{off}})$; blue solid line, magnetically induced nuclear exciton echo with $\mathbf{B}_1(204.3\ \text{ns} > t > T_{\text{on}}) = -\mathbf{B}_1(t > 204.3\ \text{ns}) = -\mathbf{B}_1(t < T_{\text{off}})$.

another approach, namely, the simple and elegant photon echo solution used in NFS experiments with SR [36–38,55,56] to allow the scattered photon to interfere with itself in the two-target setup presented in Fig. 4(a). A dynamical magnetic field $\mathbf{B}_1(t)$ is applied to target 1, and a static magnetic field $\mathbf{B}_2$ is applied to target 2. The target response is determined by $R(\alpha, \Delta_B, t) = \delta(t) - W(\alpha, \Delta_B, t)$ with $W(\alpha, \Delta_B, t) = \frac{\alpha}{\sqrt{\alpha\Gamma t}} J_1(2\sqrt{\alpha\Gamma t}) e^{-(\Gamma/2)t + i\Delta_B t}$ [31,56], and the forward-scattered x-ray field is then given by $E^{(1)}(t) = \int_0^t R(\alpha, \Delta_B, t-\tau) E^{(0)}(\tau) d\tau$ [38]. Using $E^{(0)}(t) = \delta(t)$ as x-ray input, the resulting electric field is the real part of

$$E^{(2)}(t) = \delta(t) - W(\alpha_1, \Delta_{B1}, t) - W(\alpha_2, \Delta_{B2}, t) + \int_0^t W(\alpha_2, \Delta_{B2}, t-\tau) W(\alpha_1, \Delta_{B1}, \tau) d\tau. \quad (2)$$

This depicts the interference of four possible coherent scattering channels [31,38]: (1) $\delta(t)$, no scattering; (2) $-W(\alpha_1, \Delta_{B1}, t)$, the photon is scattered by target 1 only; (3) $-W(\alpha_2, \Delta_{B2}, t)$, the photon is scattered by target 2 only; (4) the mutual integral, the photon is first scattered by target 1 and then by target 2. Channel (2) and (3) cancel each other out when the effective thicknesses of the two targets are equal $\alpha_1 = \alpha_2$ and $\mathbf{B}_1(t > T_{\text{on}}) = -\mathbf{B}_2$; i.e., $\mathbf{B}_1(t)$ is reversed at $t = T_{\text{on}}$. Hence, a significant suppression of the NFS signal can serve as a signature for the effective π phase shift magnetically modulated in target 1.

In order to obtain the total scattered field intensity, we solve Eq. (1) for both targets using the scattered field of target 1 as the incoming field for target 2. Our numerical results are illustrated in Fig. 4(b). The presence of two targets results in the faster coherent decay that proceeds with effective resonant depth of $\alpha = 2$, i.e., double the thickness of each target [36]. The magnetic field in target 1 is switched off at $T_{\text{off}} = 51$ ns and back on at $T_{\text{on}} = 100$ ns. For continuous phase, the intensity of the scattered field does not change. If, however, the phase of the retrieved field is π modulated by turning on the opposite magnetic field $-\mathbf{B}_1$, the detected signal is significantly suppressed due to destructive interference between the two scattering channels. In turn, a second magnetic field rotation back at a node value $E^{(1)}(t > 100\ \text{ns}) = 0$ produces an echo due to constructive interference, as can be seen in Fig. 4(b) for the rotation of $\mathbf{B}_1(t)$ back at $t = 204.3$ ns.

This magnetically induced nuclear exciton echo itself provides another convenient solution for photon storage. A sequence of two 180° rotations of the magnetic field direction in target 1 at the quantum beat minima can lead to storage and retrieval of the x-ray photon π phase modulated. This can be experimentally achieved in antiferromagnets as $^{57}FeBO_3$ with strong intrinsic hyperfine magnetic fields that can be rotated with the help of a weak 10 G external field [34]. Fast 180° magnetic field rotations in such materials have been demonstrated [48]. This specific case of magnetic switching in a two-target setup preserves the photon polarization and can modulate the photonic phase but is less robust compared to our scheme since both the efficiency of the storage and the phase of the released photon depend on the rotation moment. Nevertheless, the magnetically induced nuclear exciton echo might provide an additional experimentally accessible setup to investigate mechanical-free x-ray storage and phase modulation of a single-photon wave packet.

In conclusion, we have put forward the possibilities of phase-sensitive storage and π phase modulation for single hard-x-ray photons in an NFS setup. These x-ray coherent control tools are important milestones for optics and quantum information applications at shorter wavelengths aiming towards more compact future photonic devices.

We would like to thank R. Röhlsberger for fruitful discussions and T. Herrmannsdörfer for his advice on the generation of strong magnetic fields.

*Wen-Te.Liao@mpi-hd.mpg.de
†Palffy@mpi-hd.mpg.de

[1] G. E. Moore, Proc. IEEE **86**, 82 (1998).
[2] A. Politi, M. J. Martin, J. Cryan, J. G. Rarity, S. Yu, and J. L. O'Brien, Science **320**, 646 (2008).

[3] S. Kneip, C. McGuffey, J. L. Martins, S. F. Martins, C. Bellei, V. Chvykov, F. Dollar, R. Fonseca, C. Huntington, G. Kalintchenko *et al.*, Nat. Phys. **6**, 980 (2010).

[4] M. Fuchs, R. Weingartner, A. Popp, Z. Major, S. Becker, J. Osterhoff, I. Cortrie, B. Zeitler, R. Hörlein, G. D. Tsakiris *et al.*, Nat. Phys. **5**, 826 (2009).

[5] M. C. Chen, P. Arpin, T. Popmintchev, M. Gerrity, B. Zhang, M. Seaberg, D. Popmintchev, M. M. Murnane, and H. C. Kapteyn, Phys. Rev. Lett. **105**, 173901 (2010).

[6] H. P. Specht, J. Bochmann, M. Mücke, B. Weber, E. Figueroa, D. L. Moehring, and G. Rempe, Nature Photon. **3**, 469 (2009).

[7] Yu. Shvyd'ko, *X-Ray Optics: High-Energy-Resolution Applications* (Springer-Verlag, Berlin, 2004).

[8] Yu. Shvyd'ko, S. Stoupin, A. Cunsolo, A. H. Said, and X. Huang, Nat. Phys. **6**, 196 (2010).

[9] Yu. Shvyd'ko, S. Stoupin, V. Blank, and S. Terentyev, Nature Photon. **5**, 539 (2011).

[10] S.-Y. Chen, H.-H. Wu, Y.-Y. Chang, Y.-R. Lee, W.-H. Sun, S.-L. Chang, Yu. P. Stetsko, M.-T. Tang, M. Yabashi, and T. Ishikawa, Appl. Phys. Lett. **93**, 141 105 (2008).

[11] F. Pfeiffer, C. David, M. Burghammer, C. Riekel, and T. Salditt, Science **297**, 230 (2002).

[12] A. Jarre, C. Fuhse, C. Ollinger, J. Seeger, R. Tucoulou, and T. Salditt, Phys. Rev. Lett. **94**, 074801 (2005).

[13] K.-D. Liss, R. Hock, M. Gomm, B. Waibel, A. Magerl, M. Krisch, and R. Tucoulou, Nature (London) **404**, 371 (2000).

[14] Yu. V. Shvyd'ko, M. Lerche, H.-C. Wille, E. Gerdau, M. Lucht, H. D. Rüter, E. E. Alp, and R. Khachatryan, Phys. Rev. Lett. **90**, 013904 (2003).

[15] S.-L. Chang, Yu. P. Stetsko, M.-T. Tang, Y.-R. Lee, W.-H. Sun, M. Yabashi, and T. Ishikawa, Phys. Rev. Lett. **94**, 174801 (2005).

[16] C. Buth, R. Santra, and L. Young, Phys. Rev. Lett. **98**, 253001 (2007).

[17] B. Dromey *et al.*, Nat. Phys. **5**, 146 (2009).

[18] D. C. Yost, T. R. Schibli, J. Ye, J. L. Tate, J. Hostetter, M. B. Gaarde, and K. J. Schafer, Nat. Phys. **5**, 815 (2009).

[19] S. Shwartz and S. E. Harris, Phys. Rev. Lett. **106**, 080501 (2011).

[20] E. P. Kanter *et al.*, Phys. Rev. Lett. **107**, 233001 (2011).

[21] N. Rohringer *et al.*, Nature (London) **481**, 488 (2012).

[22] O. Kocharovskaya, R. Kolesov, and Y. Rostovtsev, Phys. Rev. Lett. **82**, 3593 (1999).

[23] R. Coussement *et al.*, Phys. Rev. Lett. **89**, 107601 (2002).

[24] T. J. Bürvenich, J. Evers, and C. H. Keitel, Phys. Rev. Lett. **96**, 142501 (2006).

[25] W.-T. Liao, A. Pálffy, and C. H. Keitel, Phys. Lett. B **705**, 134 (2011).

[26] J. Arthur *et al.*, *Linac Coherent Light Source (LCLS). Conceptual Design Report* (SLAC, Stanford, CA, 2002).

[27] XFEL@SACLA (2012), http://xfel.riken.jp/eng/sacla/.

[28] M. Altarelli *et al.*, *XFEL: The European X-Ray Free-Electron Laser. Technical Design Report* (DESY, Hamburg, 2006).

[29] U. Van Bürck, Hyperfine Interact. **123–124**, 483 (1999).

[30] Yu. V. Shvyd'ko, Hyperfine Interact. **125**, 173 (2000).

[31] R. Röhlsberger, *Nuclear Condensed Matter Physics with Synchrotron Radiation: Basic Principles, Methodology and Applications* (Springer-Verlag, Berlin, 2004).

[32] R. Röhlsberger, K. Schlage, B. Sahoo, S. Couet, and R. Rüffer, Science, **328**, 1248 (2010).

[33] R. Röhlsberger, H. C. Wille, K. Schlage, and B. Sahoo, Nature (London) **482**, 199 (2012).

[34] Yu. V. Shvyd'ko *et al.*, Phys. Rev. Lett. **77**, 3232 (1996).

[35] A. Pálffy, C. H. Keitel, and J. Evers, Phys. Rev. Lett. **103**, 017401 (2009).

[36] G. V. Smirnov, U. van Bürck, J. Arthur, S. L. Popov, A. Q. R. Baron, A. I. Chumakov, S. L. Ruby, W. Potzel, and G. S. Brown, Phys. Rev. Lett. **77**, 183 (1996).

[37] H. Jex, A. Ludwig, F. J. Hartmann, E. Gerdau, and O. Leupold, Europhys. Lett. **40**, 317 (1997).

[38] G. V. Smirnov, U. van Bürck, W. Potzel, P. Schindelmann, S. L. Popov, E. Gerdau, Yu. V. Shvyd'ko, H. D. Rüter, and O. Leupold, Phys. Rev. A **71**, 023804 (2005).

[39] J. Feldhaus, E. L. Saldin, J. R. Schneider, E. A. Schneidmiller, and M. V. Yurkov, Opt. Commun. **140**, 341 (1997).

[40] E. L. Saldin, E. A. Schneidmiller, Yu. V. Shvyd'ko, and M. V. Yurkov, Nucl. Instrum. Methods Phys. Res., Sect. A **475**, 357 (2001).

[41] K.-J. Kim, Yu. Shvyd'ko, and S. Reiche, Phys. Rev. Lett. **100**, 244802 (2008).

[42] M. D. Crisp, Phys. Rev. A **1**, 1604 (1970).

[43] Yu. V. Shvyd'ko, Phys. Rev. B **59**, 9132 (1999).

[44] M. O. Scully and M. S. Zubairy, *Quantum Optics* (Cambridge University Press, Cambridge, England, 2006).

[45] A. Pálffy, J. Evers, and C. H. Keitel, Phys. Rev. C **77**, 044602 (2008).

[46] Yu. V. Shvyd'ko, U. van Bürck, W. Potzel, P. Schindelmann, E. Gerdau, O. Leupold, J. Metge, H. D. Rüter, and G. V. Smirnov, Phys. Rev. B **57**, 3552 (1998).

[47] Yu. V. Shvyd'ko and U. Van Bürck, Hyperfine Interact. **123–124**, 511 (1999).

[48] Yu. V. Shvyd'ko, Hyperfine Interact. **90**, 287 (1994).

[49] Yu. V. Shvyd'ko, T. Hertrich, J. Metge, O. Leupold, E. Gerdau, and H. D. Rüter, Phys. Rev. B **52**, R711 (1995).

[50] A. Pálffy and J. Evers, J. Mod. Opt. **57**, 1993 (2010).

[51] N. Miura, T. Osada, and S. Takeyama, J. Low Temp. Phys. **133**, 139 (2003).

[52] R. Röhlsberger, T. S. Toellner, W. Sturhahn, K. W. Quast, E. E. Alp, A. Bernhard, E. Burkel, O. Leupold, and E. Gerdau, Phys. Rev. Lett. **84**, 1007 (2000).

[53] Y. Hasegawa, Y. Yoda, K. Izumi, T. Ishikawa, S. Kikuta, X. W. Zhang, and M. Ando, Phys. Rev. Lett. **75**, 2216 (1995).

[54] Y. Hasegawa and S. Kikuta, Hyperfine Interact. **123–124**, 721 (1999).

[55] P. Helistö, E. Ikonen, T. Katila, and K. Riski, Phys. Rev. Lett. **49**, 1209 (1982).

[56] P. Helistö, I. Tittonen, M. Lippmaa, and T. Katila, Phys. Rev. Lett. **66**, 2037 (1991).